Available online at www.sciencedirect.com
ScienceDirect
Applied Surface Science 252 (2006) 8624–8629
applied surface science
www.elsevier.com/locate/apsusc

# Growth of Rh nanoclusters on $TiO_2$(1 1 0): XPS and LEIS studies

László Óvári, János Kiss *

*Reaction Kinetics Research Group of the Hungarian Academy of Sciences, University of Szeged, P.O. Box 168, H-6701 Szeged, Hungary*

Received 5 November 2005; received in revised form 29 November 2005; accepted 29 November 2005
Available online 6 January 2006

**Abstract**

Rhodium clusters were prepared by evaporation on a nearly stoichiometric $TiO_2$(1 1 0) surface. The growth of metal nanoparticles, as a function of rhodium coverage, could be followed by monitoring the Rh $3d_{5/2}$ XP peak position and by low energy ion scattering spectroscopy (LEIS). The substrate temperature in the 160–300 K regime during evaporation significantly influences the cluster size, leading to smaller crystallites at low temperature. Annealing the surface results in the agglomeration of rhodium, which commenced at lower temperature for smaller clusters. At high temperatures (~900 K) encapsulation of rhodium also occurred.


*PACS:* 81.16.Dn

*Keywords:* Titania; Model catalysis; Rhodium nanoclusters; X-ray photoelectron spectroscopy; Low energy ion scattering spectroscopy

## 1. Introduction

Metal nanoclusters, deposited on oxide single crystals are important model systems for the understanding of catalytic reactions, because the morphology is quite similar to ''real'' catalysts, but the system remains well characterized [1,2]. Beyond morphology, electronic interaction between oxide supports and metal clusters is a subject of intensive research since early studies [3]. Titania is one of the most thoroughly investigated support surfaces, because – after a slight reduction in ultrahigh vacuum (UHV) – its conductivity is sufficient to avoid sample charging during electron and ion spectroscopic measurements, and scanning tunneling microscopy (STM) can also be performed [4]. The applications of titania are widespread including catalysis, photocatalysis, gas sensing, electronics, etc. As regards the catalytic aspect it is extremely important to investigate morphological characteristics of metal clusters supported on titania single crystal surfaces.

According to STM studies, the growth mode of Rh follows the Volmer–Weber mechanism on $TiO_2$(0 0 1) [5] and also on the reconstructed $TiO_2$(1 1 0)–(1 × 2) surface [6]: at room temperature three-dimensional (3D) clusters grow even at submonolayer coverages. On the non-reconstructed $TiO_2$(1 1 0), the growth mode of other group VIIIA metals, such as platinum [7] and palladium [8,9] was found to be Volmer–Weber like, too, though for Pd 2D clusters were identified at very low coverages (~0.01 ML) [9]. At low coverages (≤0.1 ML) two-dimensional growth was found even for gold, which is a typical Volmer–Weber metal [10]. Based on these data, it is very probable that Rh also forms three-dimensional particles on $TiO_2$(1 1 0) at moderate and high coverages. Accordingly, previous X-ray photoelectron spectroscopic (XPS) studies did not indicate strong interaction between rhodium and the support upon evaporation at 300 K substrate temperature [11]. The wetting ability of an overlayer metal is mostly determined by its reactivity toward oxygen [4].

Heating the Rh/$TiO_2$ model catalyst above room temperature in UHV, one may expect two morphological changes: agglomeration of metal clusters and encapsulation of metal nanoparticles by a reduced $TiO_x$ layer. The mechanism of sintering is quite frequently supposed to be Ostwald ripening: in this scenario the mass transport is realized by the migration of individual atoms detached from clusters. An alternative way is coalescence by cluster migration, which was demonstrated by

* Corresponding author. Tel.: +36 62 544 803; fax: +36 62 420 678.
*E-mail address:* jkiss@chem.u-szeged.hu (J. Kiss).

0169-4332/$ – see front matter © 2005 Elsevier B.V. All rights reserved.
doi:10.1016/j.apsusc.2005.11.081

STM for small clusters (~10 atoms) on $Pd/TiO_2(1\,1\,0)$ even at room temperature [12]. A slow aggregation of the smallest metal crystallites (2–6 atoms) at room temperature was observed also on $Rh/TiO_2(1\,1\,0)$–$(1 \times 2)$ [6], but larger crystallites (>3 nm) were immobile even at 1100 K [13]. Encapsulation in UHV depends strongly on the defect density of the titania support [11] and occurs typically in the temperature range of 500–900 K [6,14].

In this work we investigated, how the substrate temperature during evaporation influences the Rh cluster formation, because in all previous works the $TiO_2$ sample was kept at room temperature while rhodium was evaporated. For simplicity of phrasing, in the remainder of this work the temperature of the substrate during metal evaporation will be referred to as the temperature of evaporation or as the temperature of deposition.

## 2. Experimental procedure

The measurements were performed in a UHV system (base pressure $5 \times 10^{-10}$ mbar) equipped with Auger electron spectroscopy (AES), XPS, low energy ion scattering spectroscopy (LEIS) and mass spectrometry (MS). The experimental setup is described elsewhere [15,16]. Briefly, AES and XPS spectra were obtained with the same Leybold EA10/100 hemispherical analyzer, which was also used for LEIS measurements, but with the polarity of the voltage biases inverted in order to detect $He^+$ ions. XPS measurements were carried out with a constant 100 eV pass energy, using an Al Kα X-ray anode. Photoelectrons were collected at 17° (off normal) emission angle. The binding energy scale was referenced to the position of the Rh $3d_{5/2}$ peak of a thick rhodium film, taken to be 307.2 eV, based on previous results on metallic rhodium [17–20]. In LEIS measurements, $He^+$ ions of 800 eV kinetic energy were used at an ion fluence per each spectrum equal to $1.25 \times 10^{14}$ ions/cm$^2$. The scattering angle was 95°, the incident angle and the angle of detection were 50° (off normal).

The $TiO_2(1\,1\,0)$ single crystal was a product of PI-KEM. The sample was attached to a Ta plate with an oxide glue (AREMCO), and could be heated by a W filament placed behind the Ta plate. The sample could be cooled with liquid $N_2$ to 160 K, measured by a chromel–alumel thermocouple, attached to the side of the sample by the same glue.

The new colorless and transparent crystal was first annealed in UHV at 800 K for 2 h. A routine cleaning cycle consisted of $Ar^+$ bombardment (2 keV, $3 \times 10^{-6}$ A/cm$^2$, 300 K, 2 h), heating in UHV to 900 K, and oxidation in $O_2$ ($10^{-7}$ mbar) at 900 K for 10 min. The sample was then cooled down in $O_2$ to 600 K and in UHV to room temperature. The heating and cooling rates during cleaning – and in all measurements presented here – were always 2 K/s. After many of such cycles, the color of the crystal turned blue. It is known from previous STM investigations made in our group that similar treatments result basically in a $(1 \times 1)$ structure [11], but the presence of some defect sites is probable [4], as indicated also by our XPS results. $(1 \times 2)$ reconstruction of $TiO_2(1\,1\,0)$ does not occur at these relatively low temperatures. The contamination level was below the detection limit of AES.

An EGN4 e-beam evaporator of Oxford Applied Research was used for the deposition of Rh. The surface concentration of rhodium is given in close-packed monolayer equivalent (ML), which corresponds to $1.6 \times 10^{15}$ atoms/cm$^2$. The evaporation rate was 0.3 ML/min, determined by XPS. For the coverage calculation, photoelectric cross-sections of Scofield [21] and inelastic mean free paths (imfp) obtained from the TPP-2M equations [22] were used. The imfp's in titania for Ti 2p and O 1s photoelectrons were 2.17 and 2.04 nm, respectively. The imfp's for the Rh 3d, Ti 2p and O 1s photoelectrons in rhodium clusters were 1.57, 1.43 and 1.35 nm, respectively. The coverage calculation was performed at a small rhodium coverage (0.2 ML) and low deposition temperature (170 K), where clusters are smaller (see below) in order to decrease the error in the coverage determination caused by the uncertainty in cluster size.

## 3. Results and discussion

### 3.1. XPS studies

First the effect of the cleaning procedure on the reduction state of titania was investigated with XPS. The behavior of a "new" crystal was different from that of a "blue" sample (obtained after ca. 30 cleaning cycles). (After mounting the sample in the XPS system, it was first annealed in UHV at 800 K for 2 h and one cleaning cycle, consisting of $Ar^+$ bombardment at 300 K, annealing and oxidation at 900 K, was performed. After such a treatment the surface was clean, according to AES. That state is defined as "new" sample.) The second Ar ion bombardment of the new crystal led to the substantial reduction of the surface by the preferential removal of O. In the Ti 2p region (Fig. 1) significant amount of reduced ($Ti^{3+}$ and $Ti^{2+}$) states can be seen beside the $Ti^{4+}$ peak. The assignment of peak positions was made based on literaure data (Table 1).

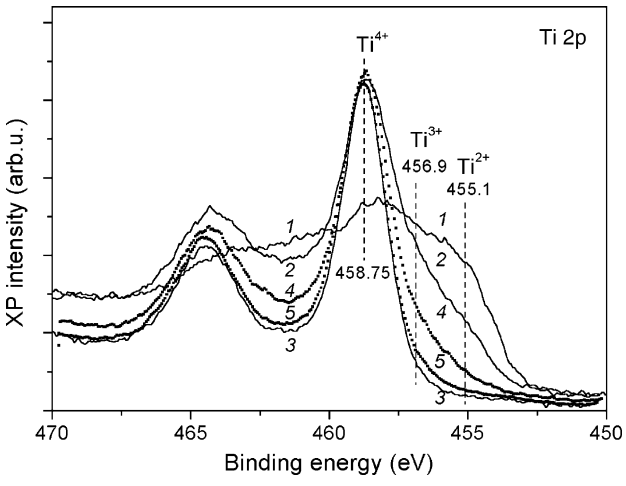


Fig. 1. Ti 2p XP spectra collected after various treatments performed on a "new" $TiO_2(1\,1\,0)$ sample (solid lines) and on a "blue" sample (dotted lines): a new sample after $Ar^+$ bombardment (300 K, 2 keV, $1.35 \times 10^{17}$ ions/cm$^2$) (1), followed by annealing to 800 K (2) and 900 K (3) in UHV; a blue sample after $Ar^+$ bombardment – as for (1) – followed by annealing to 900 K in UHV (4), followed by oxidation in $O_2$ ($10^{-7}$ mbar, 10 min) at 900 K (5). In the last case $O_2$ was evacuated after cooling the sample to 600 K. All spectra were collected at room temperature.

Table 1
Characteristic Ti $2p_{3/2}$ binding energies (eV) for different oxidation states of titanium

| $Ti^{4+}$ | $Ti^{3+}$ (refer to $Ti^{4+}$) | $Ti^{2+}$ (refer to $Ti^{4+}$) | Reference |
|---|---|---|---|
| 458.8 | | | [11] |
| 458.6 | | | [7] |
| | −1.7 | −3.8 | [23] |
| 458.8 | −1.7 | −3.4 | [24] |

Heating the $Ar^+$ bombarded new sample to 800 K led to a significant simplification of the Ti 2p XPS feature. It was dominated by the $Ti^{4+}$ component, but a rather strong tail at lower binding energies, originated by the reduced Ti components, was still present. Annealing further in UHV at 900 K was sufficient to remove (almost) completely the tail at low binding energies, which means that the surface of the new sample was (almost) stoichiometric after such treatments.

Annealing of a blue sample at 900 K in UHV after $Ar^+$ bombardment did not result in a stoichiometric surface (Fig. 1). Oxidation at 900 K, however, led to a significant diminution of the reduced components, but did not result in their complete removal, indicating the presence of some defect sites. Investigations on the Rh nanoparticle growth presented below were performed on such an oxidized blue sample.

The Rh 3d doublet as a function of the amount of rhodium deposited keeping the titania sample at room temperature is depicted in Fig. 2A. A 0.5 eV shift of the Rh $3d_{5/2}$ peak position toward lower binding energies was observed with increasing coverage. On the other hand, deposition of Rh did not exert detectable influence on the peak shape of the Ti 2p feature (not shown), suggesting only a weak interaction between Rh and titania. In this way, the shift of the rhodium peak is basically not a charge transfer effect between the oxide support and metal nanopartcicles, but is very probably related to the change in electronic screening as a function of cluster size. As Rh particles grow in size, a bulklike state is reached with a more metallic electronic system, resulting in a more efficient screening (a final-state effect). Similar core-level shifts were observed in the same direction for $Cu/TiO_2$(1 1 0) [25], $Cu/Al_2O_3$ [26], $Pt/TiO_2$(1 1 0) [7], $Rh/TiO_2$(1 1 0) [11] and for gold supported on relatively inert surfaces, such as amorphous C, $SiO_2$ or $Al_2O_3$ [27]. The lower average coordination number of smaller rhodium clusters would cause a smaller shift in the opposite direction due to band narrowing, but this initial-state effect is overwhelmed by the strong, countervailing final-state effect [28]. At higher coverages the Rh 3d doublet was slightly asymmetric toward higher binding energies, which is also a characteristic of metal cluster size increase. For larger clusters, as the electronic system becomes more metallic, photoelectrons can excite electron–hole pairs before leaving the sample, resulting in a small kinetic energy loss and in the asymmetry [28].

When rhodium was deposited at low temperature (160 K), a much larger shift (0.8 eV) in the Rh $3d_{5/2}$ binding energy was observed (Fig. 2B). The final value obtained at 4 ML (characteristic of the bulk metal) was independent of the deposition temperature. At small coverages (up to ∼1.5 ML), however, the observed higher binding energies indicate the formation of smaller metal clusters. Dependence of the Rh $3d_{5/2}$ peak positions on the deposition temperature, as a function of metal coverage, is also shown in Fig. 3A.

In Fig. 3B, rhodium binding energies as a function of annealing in UHV at different temperatures are displayed. Annealing the 0.3 ML metal overlayer, deposited at room temperature, to $T \geq 500$ K led to a gradual shift toward lower binding energies, very probably due to agglomeration of metal clusters. The bulk value is reached after annealing at 700 K. It does not mean that the cluster size is not growing further due to annealing at 900 K. It is clear that the Rh $3d_{5/2}$ binding energy is

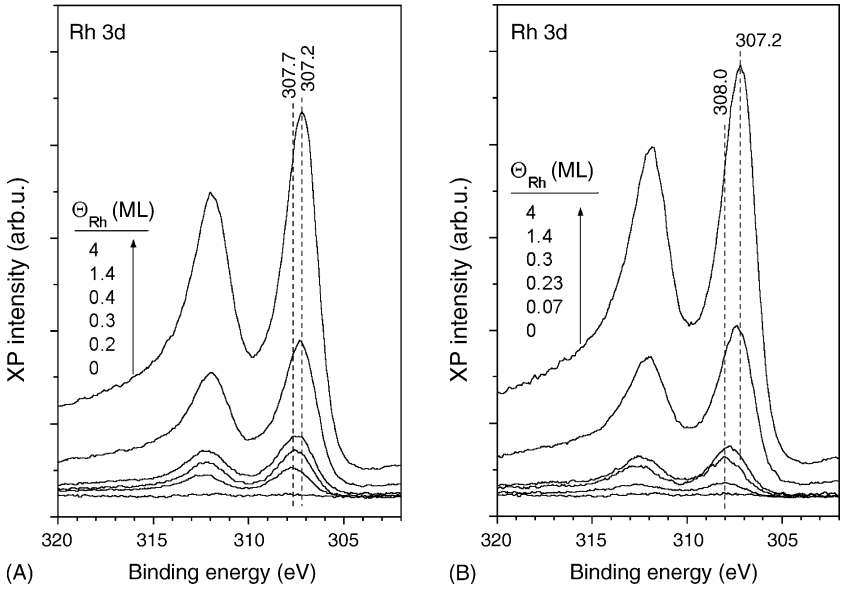


Fig. 2. Rh 3d XP spectra as a function of rhodium coverage at $T_{evap} = 300$ K (A) and $T_{evap} = 160$ K (B) evaporation temperatures. Spectra were collected at the temperature of evaporation.

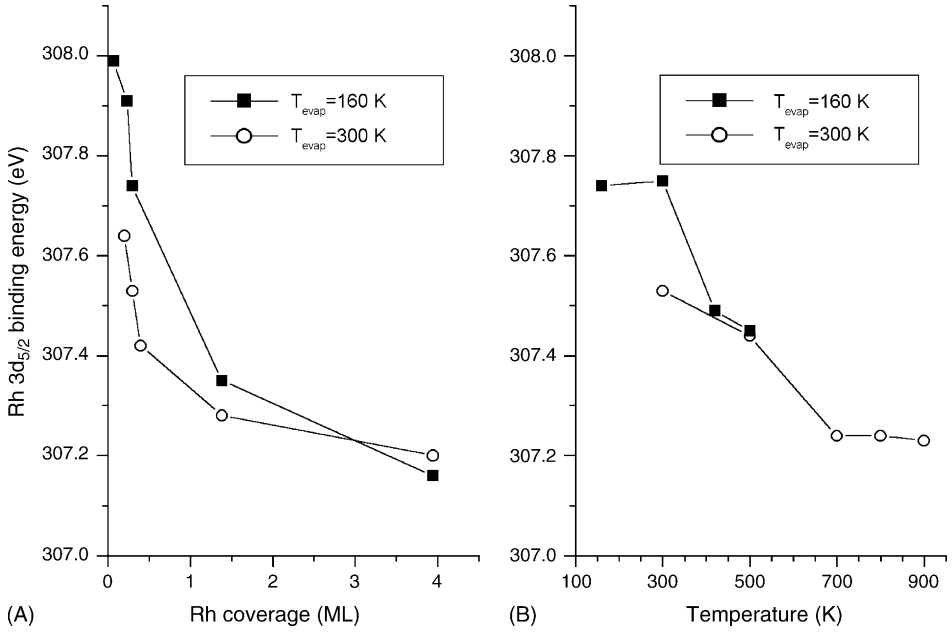


Fig. 3. (A) Rh $3d_{5/2}$ binding energy at increasing coverage of rhodium deposited at different temperatures and (B) Rh $3d_{5/2}$ binding energy after annealing the 0.3 ML $Rh/TiO_2(1\ 1\ 0)$ surface to different temperatures for 1 min.

sensitive to the nanoparticle size only for small clusters, having an electronic structure significantly different from the bulk. For large clusters the bulk value should be obtained. Encapsulation of rhodium may contribute to binding energy changes. Note, however, that encapsulation of Pt particles by titania led to a slight shift of the Pt 4f doublet toward higher binding energies [29], suggesting that the negative shifts observed in our case during annealing are not a consequence of the decoration of metal nanoclusters by the oxide. It was also checked by ion scattering spectroscopy (see below).

When Rh was deposited at 160 K, subsequent annealing to room temperature exerted no influence on the Rh $3d_{5/2}$ peak position (Fig. 3B). The cluster size obtained this way is smaller than after evaporation at 300 K. This effect of the evaporation temperature can be rationalized by the lower diffusion rate of Rh atoms during evaporation at 160 K, leading to smaller nanoparticles. The clusters formed are probably stable up to room temperature, because migration of clusters is much slower than migration of atoms (during evaporation). Very slow agglomeration of rhodium clusters was observed by STM at room temperature on the time scale of 12 h, but only for coverages $\Theta_{Rh} \sim 0.01$ ML, when very small crystallites form (2–6 atoms) [6]. The onset of agglomeration of the crystallites formed at 160 K was detected at 400–500 K (Fig. 3B).

### 3.2. LEIS studies

Changes in the Rh and Ti ion scattering peak areas as a function of Rh coverage are displayed in Fig. 4 at different deposition temperatures. Low energy ion scattering spectroscopy is sensitive almost exclusively to the topmost layer if noble gas ions are used. Consequently, the deposition of rhodium resulted in the diminution of titanium and oxygen peaks due to the shadowing effect of metal clusters. Substrate peaks, however, were well detectable even in the presence of several monolayer equivalents of rhodium, which is a clear symptom of Volmer–Weber growth. Deposition of the metal on the oxide at 160 K led to steeper changes in the rhodium and substrate intensities, if compared to evaporation at room temperature. It indicates, in accordance with our XPS results, the formation of smaller crystallites at low temperature.

To get a basic idea of cluster size, the diameter of metal nanoparticles was estimated from LEIS results. For this estimation the following assumptions were made: (1) the fraction of the surface covered by rhodium corresponded to the relative decrease in the titanium peak area with respect to the titanium intensity obtained for the clean oxide surface; (2) the clusters have ellipsoidal shape with circular footprint; (3) all clusters have the same diameter; (4) the aspect ratio was assumed to be 1/3, based on previous STM results [5,6]. Cluster diameters estimated this way for cluster formation at room temperature

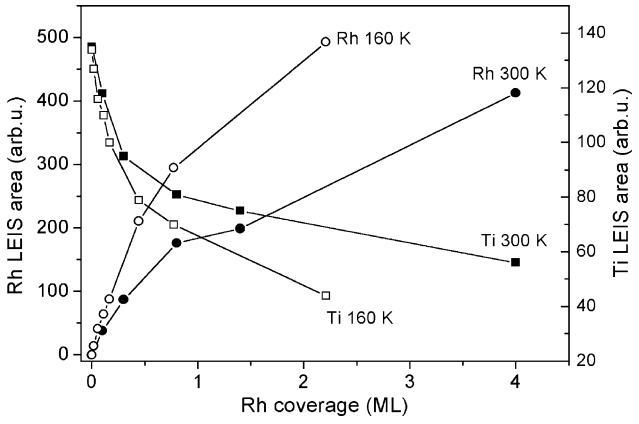


Fig. 4. Rh and Ti ion scattering peak areas as a function of Rh coverage at 160 and 300 K evaporation temperatures.

were 0.9 and 3.1 nm at 0.15 and 1.4 ML of rhodium, respectively, in reasonable agreement with previous STM studies on $TiO_2$(0 0 1) [5] and $TiO_2$(1 1 0)–(1 × 2) [6]. At the same metal coverages, lowering the evaporation temperature to 160 K led to a decrease in cluster size to 0.6 and 2.3 nm, respectively.

The possible role of encapsulation in the shifts of the Rh $3d_{5/2}$ XP peak was investigated by LEIS, too (Fig. 5). Evaporation of 0.8 ML of Rh at 300 K caused the appearance of the Rh peak, and a reduction of the Ti (and O) signal, due to the shadowing effect of metal clusters. Only slight changes were observed after subsequent annealing at $T \leq 600$ K. (The small increase in the Rh intensity at 600 K is very probably caused by the desorption of background gases.) Annealing to 700 K resulted in the diminution of the Rh peak and an enlargement of the Ti peak. These changes were even more significant at higher temperatures, leading to the complete disappearance of the Rh peak at 900 K.

Both agglomeration and encapsulation of metal clusters should lead to the diminution of the Rh peak and to the increase in the Ti peak. The complete encapsulation of metal clusters, however, results in the total disappearance of the metal signal, which is a direct consequence of the topmost layer sensitivity of LEIS, and was observed during the encapsulation of Pt by $TiO_2$ [29]. At 700 K we found only a small decrease in the Rh signal, implying that encapsulation must be very limited, if it proceeds at all. Based on this fact, we feel safe to conclude that the shift of the Rh $3d_{5/2}$ binding energy observed between 500 and 700 K (Fig. 3B) can be assigned to the agglomeration of Rh clusters. Note, however, that annealing the 0.8 ML Rh/$TiO_2$(1 1 0) surface at 700 K for much longer periods (1–2 h) produces a more dramatic Rh ion scattering signal decrease (not shown), though the disappearance of the metal peak was not observed. In this case the occurrence of more significant encapsulation cannot be excluded.

The complete absence of the Rh peak after annealing at 900 K for 1 min (Fig. 5) is a clear sign of the complete encapsulation of rhodium by the oxide. An alternative explanation for the disappearance of Rh signal might be that all the rhodium diffused into the bulk of titania. This is ruled out by the fact that annealing at 900 K decreased only slightly the area of the Rh 3d doublet (inset of Fig. 5). Moreover, it seems improbable that the binding energy of rhodium atoms located in the oxide lattice would coincide with the binding energy of bulk metallic rhodium.

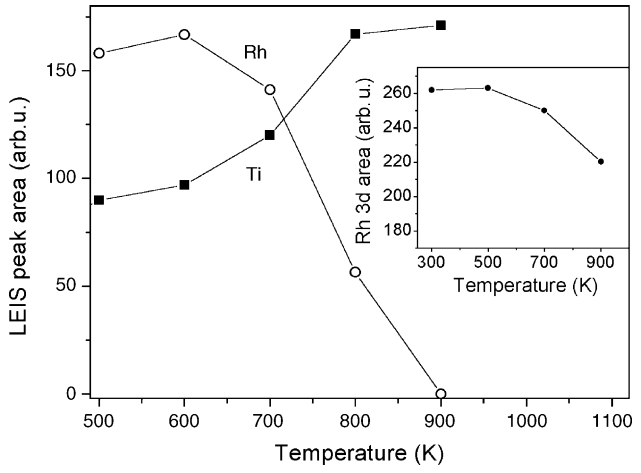


Fig. 5. Rh and Ti LEIS peak areas obtained after annealing the 0.8 ML Rh/$TiO_2$ surface to different temperatures for 1 min. Rhodium was deposited at 300 K. Inset: area of the Rh 3d XP doublet after annealing to different temperatures.

The disapperance of Rh LEIS signal at 900 K might be also explained in a third way: if metallic clusters agglomerated into a few very large nanoparticles then rhodium ion scattering signal might decrease below the detection limit. In our case a rhodium LEIS peak with an intensity corresponding to one percentage of the peak observed at 300–600 K would be at the limit of detection. Assuming no encapsulation, only agglomeration (with no change in the nanoparticle shape), approximately a 100-fold increase in the cluster diameter should occur leading to that small metal peak, taking into account that the area of the nanoparticle footprint (approximately proportional to the LEIS intensity of one Rh cluster) changes with the square of the diameter, while the cluster volume (inversely proportional to the nanoparticle density) changes with its cube. Such a giant increase in the cluster size can be ruled out based on previous STM results made in our laboratory [6,11], leading us to conclude that the complete absence of the Rh ion scattering peak at 900 K is a consequence of encapsulation.

Note, that the Ti intensity observed after 900 K annealing was slightly higher than that observed for the pure oxide, while the oxygen intensity was slightly smaller for the encapsulated surface. It is in agreement with previous results indicating that the encapsulating phase is a reduced titanium-oxide layer [4].

## 4. Conclusion

The $TiO_2$(1 1 0) surface, used as a support for these measurements was nearly stoichiometric, with a small amount of defect sites. XPS and LEIS results indicated that the size of the rhodium clusters, produced by evaporation, increased as a function of coverage. The temperature of the evaporation can also be used to influence cluster size, leading to smaller nanoparticles at low temperature (160 K). Annealing the Rh/$TiO_2$(1 1 0) surface to higher temperatures led to the agglomeration and encapsulation of metal clusters. The onset of agglomeration depended also on the cluster size, i.e. on the evaporation temperature.

## Acknowledgements

This work was supported by grants OTKA T46351 and T43057 and by grant NKFP 3A058-04 of the Ministry of Education. The authors would like to thank Dr. A. Berkó and R. Németh for fruitful discussions.

## References

[1] C.R. Henry, Surf. Sci. Rep. 31 (1998) 231.
[2] H.-J. Freund, Surf. Sci. 500 (2002) 271.
[3] F. Solymosi, Catal. Rev. 1 (1968) 233.
[4] U. Diebold, Surf. Sci. Rep. 48 (2003) 53 (and references therein).

[5] G.E. Poirier, B.K. Hance, J.M. White, J. Phys. Chem. 97 (1993) 5965.
[6] A. Berkó, G. Ménesi, F. Solymosi, Surf. Sci. 372 (1997) 202.
[7] H.-P. Steinrück, F. Pesty, L. Zhang, T.E. Madey, Phys. Rev. B 51 (1995) 2427.
[8] T.E. Madey, in: D.A. King, D.P. Woodruff (Eds.), The Chemical Physics of Solid Surfaces and Heterogeneous Catalysis, vol. 8, Elsevier, Amsterdam, 1997.
[9] C. Xu, X. Lai, G.W. Zajac, D.W. Goodman, Phys. Rev. B 56 (1997) 13464.
[10] S.C. Parker, A.W. Grant, V.A. Bondzie, C.T. Campbell, Surf. Sci. 441 (1999) 10.
[11] A. Berkó, I. Ulrych, K.C. Prince, J. Phys. Chem. B 102 (1998) 3379.
[12] M.J.J. Jak, C. Konstapel, A. van Kreuningen, J. Verhoeven, J.W.M. Frenken, Surf. Sci. 457 (2000) 295.
[13] A. Berkó, F. Solymosi, Surf. Sci. 400 (1998) 281.
[14] H.R. Sadeghi, V.E. Heinrich, Appl. Surf. Sci. 19 (1984) 330.
[15] L. Óvári, J. Kiss, A.P. Farkas, F. Solymosi, J. Phys. Chem. B 109 (2005) 4638.
[16] L. Óvári, J. Kiss, A.P. Farkas, F. Solymosi, Surf. Sci. 566–568 (2004) 1082.
[17] L.A. DeLouise, E.J. White, N. Winograd, Surf. Sci. 147 (1984) 252.
[18] R. Nyholm, N. Martensson, J. Phys. C 13 (1980) L279.
[19] C.D. Wagner, W.M. Riggs, L.E. Davis, J.F. Moulder, G.E. Muilenberg (Eds.), Handbook of X-ray Photoelectron Spectroscopy, vol. 55344, Perkin-Elmer Corporation, Physical Electronics Division, Eden Prairie, MN, 1979.
[20] P.S. Wehner, P.N. Mercer, G. Apai, J. Catal. 84 (1983) 244.
[21] J.H. Scofield, J. Electron Spectrosc. Relat. Phenom. 8 (1976) 129.
[22] S. Tanuma, C.J. Powell, D.R. Penn, Surf. Interface Anal. 21 (1994) 165.
[23] W. Göpel, J.A. Anderson, D. Frankel, M. Jaehnig, K. Phillips, J.A. Schäfer, G. Rocker, Surf. Sci. 139 (1984) 333.
[24] S. Pétigny, H. Mostefa-Sba, B. Domenichini, E. Lesniewska, A. Steinbrunn, S. Bourgeois, Surf. Sci. 410 (1998) 250.
[25] U. Diebold, J.-M. Pan, T.E. Madey, Phys. Rev. B 47 (1993) 3868.
[26] V. Di Castro, G. Polzonetti, R. Zanoni, Surf. Sci. 162 (1985) 348.
[27] M.G. Mason, Phys. Rev. B 27 (1983) 748.
[28] W.F. Egelhoff Jr., Surf. Sci. Rep. 6 (1986) 253 (and references therein).
[29] F. Pesty, H.-P. Steinrück, T.E. Madey, Surf. Sci. 339 (1995) 83.